2-1-2015

The Feasibility of Imaging Myocardial Ischemic/Reperfusion Injury Using ^{99m}Tc-labeled Duramycin in a Porcine Model

Lei Wang
Chinese Academy of Medical Science

Feng Wang
Nanjing Medical University

Wei Fang
Chinese Academy of Medical Science

Steven E. Johnson
Northwestern University

Said H. Audi
Marquette University, said.audi@marquette.edu

See next page for additional authors

Accepted version. *Nuclear Medicine and Biology*, Vol. 42, No. 2 (February 2015): 198-204. DOI.

The Feasibility of Imaging Myocardial Ischemic/Reperfusion Injury Using ^{99m}Tc-labeled Duramycin In a Porcine Model

Lei Wang
Department of Nuclear Medicine, Cardiovascular Institute & Fu Wai Hospital, Peking Union Medical College & Chinese Academy of Medical Science,
Beijing, China
Feng Wang
Department of Nuclear Medicine, Nanjing First Hospital Affiliated to Nanjing Medical University,
Nanjing, China
Wei Fang
Department of Nuclear Medicine, Cardiovascular Institute & Fu Wai Hospital, Peking Union Medical College & Chinese Academy of Medical Science,
Beijing, China
Steven E. Johnson
Department of Medicine, Division of Cardiology,
Feinberg School of Medicine, Northwestern University,
Chicago, IL

Nuclear Medicine and Biology, Vol 41, No. 2 (February 2015): pg. 198-204. DOI.

Said Audi

Department of Biomedical Engineering, Marquette University, Milwaukee, WI

Michael Zimmer

Nuclear Medicine Department, Northwestern Memorial Hospital, Chicago, IL

Thomas A. Holly

Department of Medicine, Division of Cardiology, Feinberg School of Medicine, Northwestern University, Chicago, IL

Daniel C. Lee

Department of Medicine, Division of Cardiology, Feinberg School of Medicine, Northwestern University, Chicago, IL

Bao Zhu

Department of Nuclear Medicine, Wuxi People's Hospital Affiliated to Nanjing Medical University, Wuxi, China

Haibo Zhu

State Key Laboratory of Bioactive Substance and Function of Natural Medicines, Institute of Materia Medica, Peking Union Medical College & Chinese Academy of Medical Sciences, Beijing, China

Ming Zhao

Department of Medicine, Division of Cardiology, Feinberg School of Medicine, Northwestern University, Chicago, IL

Abstract: When pathologically externalized, phosphatidylethanolamine (PE) is a potential surrogate marker for detecting tissue injuries. ^{99m}Tc-labeled duramycin is a peptide-based imaging agent that binds PE with high affinity and specificity. The goal of the current study was to investigate the clearance

Nuclear Medicine and Biology, Vol 41, No. 2 (February 2015): pg. 198-204. DOI.

kinetics of ^{99m}Tc-labeled duramycin in a large animal model (normal pigs) and to assess its uptake in the heart using a pig model of myocardial ischemia–reperfusion injury.

Methods

The clearance and distribution of intravenously injected ^{99m}Tc-duramycin were characterized in sham-operated animals (n = 5). In a closed chest model of myocardial ischemia, coronary occlusion was induced by balloon angioplasty (n = 9). ^{99m}Tc-duramycin (10–15 mCi) was injected intravenously at 1 hour after reperfusion. SPECT/CT was acquired at 1 and 3 hours after injection. Cardiac tissues were analyzed for changes associated with acute cellular injuries. Autoradiography and gamma counting were used to determine radioactivity uptake. For the remaining animals, ^{99m}Tc-tetrafosamin scan was performed on the second day to identify the infarct site.

Results

Intravenously injected ^{99m}Tc-duramycin cleared from circulation predominantly via the renal/urinary tract with an α-phase half-life of 3.6 ± 0.3 minutes and β-phase half-life of 179.9 ± 64.7 minutes. In control animals, the ratios between normal heart and lung were 1.76 ± 0.21, 1.66 ± 0.22, 1.50 ± 0.20 and 1.75 ± 0.31 at 0.5, 1, 2 and 3 hours post-injection, respectively. The ratios between normal heart and liver were 0.88 ± 0.13, 0.80 ± 0.13, 0.82 ± 0.19 and 0.88 ± 0.14. *In vivo* visualization of focal radioactivity uptake in the ischemic heart was attainable as early as 30 min post-injection. The *in vivo* ischemic-to-normal uptake ratios were 3.57 ± 0.74 and 3.69 ± 0.91 at 1 and 3 hours post-injection, respectively. Ischemic-to-lung ratios were 4.89 ± 0.85 and 4.93 ± 0.57; and ischemic-to-liver ratios were 2.05 ± 0.30 to 3.23 ± 0.78. The size of ^{99m}Tc-duramycin positive myocardium was qualitatively larger than the infarct size delineated by the perfusion defect in ^{99m}Tc-tetrafosmin uptake. This was consistent with findings from tissue analysis and autoradiography.

Conclusion

^{99m}Tc-duramycin was demonstrated, in a large animal model, to have suitable clearance and biodistribution profiles for imaging. The agent has an avid target uptake and a fast background clearance. It is appropriate for imaging myocardial injury induced by ischemia/reperfusion.

Keywords: Duramycin; Phosphatidylethanolamine; Ischemia–reperfusion injury; Apoptosis

1. Introduction

In mammalian cells, the phospholipid bilayer of the plasma membrane serves as a physical barrier with important biological functions. The pathological disruption of the bilayer can result in a scrambled phospholipid distribution with or without membrane rupturing.[1,2] The exposure of aminophospholipids such as phosphatidylserine (PS) and phosphatidylethanolamine (PE) provides surrogate markers for detecting tissue injuries. Imaging strategies that

target scrambled phospholipid bilayer in various tissues have been widely reported.[2,3,4,5,6]

There has been a continuous effort to develop positive radionuclide imaging techniques for detecting ischemic injury in the cardiovascular system.[7] This effort is geared toward a combination of robust molecular recognition mechanism, an avid target uptake, and a rapid blood clearance (preferably renal) with a low blood pool and hepatic background. These criteria are critical for cardiac imaging applications, because of large bodies of blood pool from adjacent heart cambers and close vicinity to the liver especially at the apical region of the heart. Additionally, like most diagnostic imaging procedures, it is desirable to perform the scan in a timely fashion, preferably shortly after tracer injection without a prolonged delay. In this regard, the lantibiotic duramycin is uniquely situated because of its structural features. Duramycin is currently the smallest known polypeptide that forms a stereospecific binding pocket.[8,9] It has receptor-like binding behaviors, yet peptide-like clearance kinetics.[10,11] Duramycin binds PE with a high affinity with a Kd reported at around 5 nM.[12] It was also reported that once bound to PE, the binding does not readily dissociate even in the presence of organic solvent.[12] A combination of tight binding with low molecular weight makes duramycin a candidate of interest for cardiovascular imaging applications.

The aims of the current study were to evaluate the clearance of intravenously injected ^{99m}Tc-duramycin in healthy pigs and to test the feasibility of detecting acute myocardial injury in a porcine model of coronary occlusion/reperfusion. The sarcolemma of cardiomyocytes is a rich source of PE, which when exposed at the extracellular surface provides stereospecific and abundant binding targets in conditions such as ischemic injuries.[13] In this work, we present results of studies with ^{99m}Tc-duramycin in a porcine model of ischemia. Since the porcine cardiovascular system is comparable to that of humans, these studies provide important data for assessing ^{99m}Tc-duramycin as an effective imaging agent for detecting ischemic injuries in the heart.

2. Materials and methods

Duramycin was covalently modified with succinimidyl 6-hydrazinonicotinate acetone hydrazone (HYNIC, Solulink) and purified

by HPLC as previously reported.[10] The molecular weight of HYNIC modified duramycin was confirmed using matrix-assisted laser desorption/ionization mass spectrometry. The radiopharmaceutical was prepared using a single-step kit formulation, where 740–925 MBq (20–25 mCi) technetium-99 m was injected into duramycin kit vial and heated for 20 min at 80 °C. Quality control steps, including radioHPLC and stability tests, were carried out as described before.[11,14]

2.1. Clearance studies in normal animals

The animal protocol was approved by the Institutional Animal Care and Use Committee at Nanjing First Hospital affiliated to Nanjing Medical University and at the Feinberg School of Medicine, Northwestern University. For characterizing the clearance and distribution profiles of ^{99m}Tc-duramycin, five control animals were studied. Pigs (M/F, 25–30 kg) were initially anesthetized with intramuscular injection of ketamine hydrochloride (10 mg/kg). Anesthesia was maintained using isoflurane. A balloon catheter (length 15 mm, diameter 2.5–3 mm) was delivered into the coronary branches then withdrawn without inflation as sham operated control. A dose of ^{99m}Tc-duramycin (370–555 MBq, 10–15 mCi/animal) was injected into the ear vein. Blood samples were withdrawn for gamma counting measurements at 0.5, 1, 2, 3, 4, 5, 10, 15, 30, 60, 120 and 180 minutes post-injection. Anterior whole-body planar and SPECT/CT images were acquired at 0.5, 1, 2 and 3 hr post-injection using a Symbia TruePoint hybrid SPECT/CT scanner (Siemens). The parameters for planar imaging were 140 ± 20% keV energy window, 128 x 128 matrix size, 1 million total counts. Parameters for SPECT included 140 ± 20% keV, with 6 sec acquisition per projection angle. CT was used for attenuation correction and anatomical coregistration with SPECT images. Based on blood sample gamma counting measurements, the biphasic clearance time–activity data were fit to the following two-exponential equation:

$$C_b(t) = Ae - t/\alpha + (100 - A)e - t/\beta$$

where *A* and (100 − *A*) are the factional (%) amplitudes of the two exponentials with a fast time constant *α* (fast phase) and a slow time constant *β* (slow phase), respectively. The half-lives of the α and β

phases were then determined by scaling the estimated corresponding time constants by ln(2).

2.2. Imaging myocardial injury in a porcine model of coronary occlusion and reperfusion

For the coronary occlusion group, pigs (n = 9, M/F, 25–30 kg) were anesthetized as described above. A balloon catheter (length 15 mm, diameter 2.5–3 mm) was positioned into one of the following coronary branches: distal end of the left descending coronary artery (n = 5), or left circumflex branch (n = 4). Arterial occlusion was initiated by inflating and maintaining the angioplasty balloon at 8 atmosphere pressure and lasted between 20 and 30 min. Reperfusion was initiated by deflating and withdrawal of the angioplasty balloon. Both coronary occlusion and the subsequent reperfusion were confirmed by angiography. ECG profiles typical of acute ischemic and reperfusion injury, including arrhythmia and ST segment depression or elevation, were observed. Levels of cardiac enzymes, including creatine kinase (CK) and creatine kinase MB (CKMB), were measured for validation of acute myocardial injury. At 1 hr after reperfusion, 370–555 MBq (10–15 mCi/animal) of ^{99m}Tc-duramycin was injected into the ear vein, anterior whole-body planar images were acquired at 0.5 hour post-injection. SPECT/CT images were acquired at 1 and 3 hr post-injection. Perfusion imaging was performed on the second day, at 45 min after an intravenous injection of ^{99m}Tc-tetrofosmin (370–555 MBq, 10–15 mCi/animal). Imaging data were reconstructed and processed with attenuation correction based on the acquired CT data using software provided by the manufacturer (Syngo, Siemens). SPECT data localization was validated using CT anatomical coregistration. Radioactivity uptake in regions of interests was determine at 1 and 3 hours post-injection for the myocardial wall, lung and liver in terms of counts/voxel/min. Uptake ratios between heart/lung and heart/liver were subsequently calculated.

2.3. Tissue analysis

Representative cardiac tissue specimens were harvested from the ischemic core and periphery for analysis. To quantitatively examine the extent of DNA damage of each cell, we performed flow

Nuclear Medicine and Biology, Vol 41, No. 2 (February 2015): pg. 198-204. DOI.

cytometric analysis on cardiac cells isolated from separate tissue specimens. Cardiac tissues were dissected into small pieces, and were gently pressed through a fine mesh. The cells were fixed, stained with Propidium Iodide and analyzed by flow cytometry. The presence of cells with sub-G0 DNA content was determined. This procedure was performed in 3 independent measurements using tissues from 3 different animals. Hematoxylin and eosin (H&E) staining was performed on cryosections. For ultrastructural examination, ultrathin sections were cut from core ischemic tissues on an Ultracut ultramicrotome (Mager Scientific Inc., Dexter, MI), mounted on mesh copper grids, and poststained in uranyl acetate and Reynold's lead citrate. The sections were examined using a transmission electronic microscope (JEM-1010). The presence of apoptosis was determined using tissues harvested from the periphery of ischemic regions. DNA fragmentation was analyzed by terminal deoxynucleotidytransferase mediated dUTP nick-end labeling (TUNEL) assay using a commercial kit (Maxin-Bio) according the manufacturer's protocol on 8 μm cryosections. TUNEL-positive nuclei as a percentage of total nuclei was determined and used as the apoptotic index.

2.4. Statistical analysis

All data were expressed as mean ± standard deviation; statistical analysis was performed using Student's *t*-test, where a *P* value of less than 0.05 was considered statistically significant.

3. Results

3.1. In vivo *kinetic studies in normal pigs*

The radiopharmaceutical dose consistently had a radiochemical purity at 90% or greater, and was stable without significant presence of dissociated radioactivity. After intravenous injection, ^{99m}Tc-duramycin cleared from the blood circulation with predominantly renal excretion, leaving a low systemic background including the blood pool and liver. The blood clearance profile of ^{99m}Tc-duramycin in control animals is shown in Fig. 1A. The half-life for the fast clearance phase (α-phase), which accounted for 77.6% ± 5.5% of blood activity, was estimated to be 3.6 ± 0.3 minutes (n = 5). The half-life for the slow

clearance phase (β-phase) was estimated to be 179.9 ± 64.7 minutes (n = 5). According to the SPECT data, the radioactivity uptake levels in terms of counts/voxel/min in normal heart, lung and liver, and their dynamic clearance profiles are shown in Fig. 1B. The ratios between normal heart and lung were 1.76 ± 0.21, 1.66 ± 0.22, 1.50 ± 0.20 and 1.75 ± 0.31 at 0.5, 1, 2 and 3 hours post-injection, respectively. The ratios between normal heart and liver were 0.88 ± 0.13, 0.80 ± 0.13, 0.82 ± 0.19 and 0.88 ± 0.14. Representative whole-body anterior planar images acquired at 0.5, 1, 2 and 3 hours post-injection are shown in Fig. 1C. The time series of planar images are presented with the same threshold and scale bar. Apart from the bladder signal, the cardiac blood pool and liver background was visible at 30 minutes after ^{99m}Tc-duramycin injection. These signals diminished over time to near background levels.

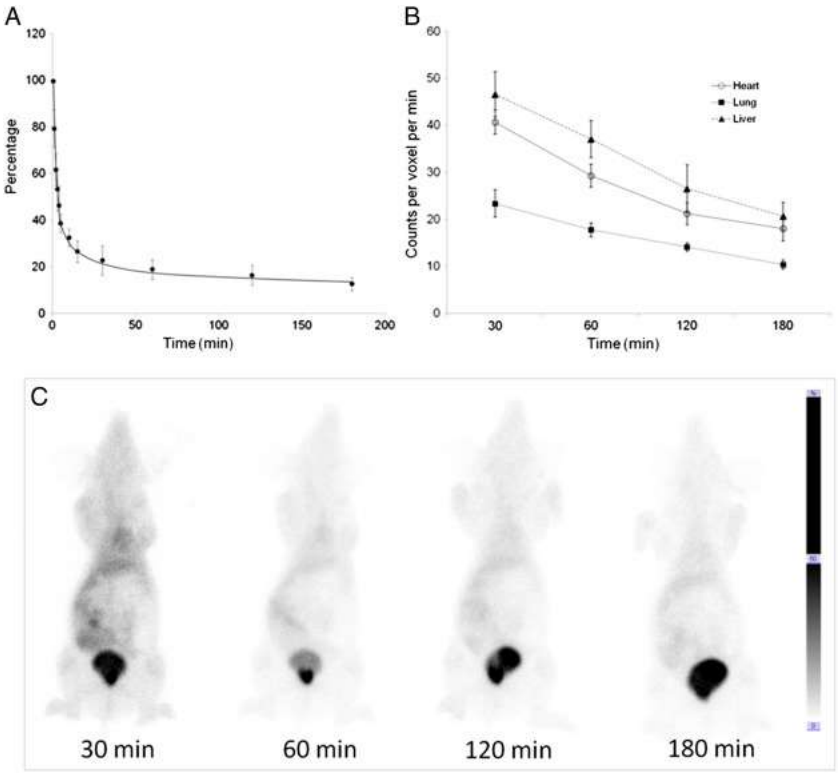

Fig. 1. ^{99m}Tc-duramycin clearance and distribution in control animals. (A) Blood clearance profile as a function of time. Solid line: two-exponential fitting for estimation of blood clearance half-lives. (B) Organ clearance profiles derived from serial SPECT data, for the heart (○), lung (■) and liver (▲) as a function of time. (C) Serial anterior whole-body planar images acquired at 30, 60, 120 and 180 minutes after intravenous ^{99m}Tc-duramycin injection.

Nuclear Medicine and Biology, Vol 41, No. 2 (February 2015): pg. 198-204. DOI.

3.2. In vivo *imaging in a porcine model of myocardial ischemia and reperfusion*

In animals that experienced myocardial ischemia and reperfusion, the presence of tissue injuries was confirmed by cardiac enzyme tests. CK level elevated from 310.3 ± 23.2 to 1793.4 ± 1451.6 ($P = 0.045$), and CKMB level increased from 44.0 ± 5.4 to 661.2 ± 281.3 ($P < 0.01$). Focal uptake at the ischemic site was clearly discernible in planar whole-body scans as early as 30 minutes after injection (Fig. 2A). In contrast, this was absent in control animals but only a diffused blood pool background (Fig. 1C). In SPECT images acquired at 1 hour post-injection, a prominent hot spot at the ischemic myocardium in the anterior left free wall was detectable, as seen in representative images (Fig. 2B and C). Radioactivity uptake in the remote, normal myocardium was at background. Signals from the blood pool in heart chambers were minimal. At 3 hours post-injection, the focal uptake remained conspicuous without washout (Fig. 3A and B). In ^{99m}Tc-tetrafosamin scan acquired on day 2 the perfusion deficiency was found at the same location as the ^{99m}Tc-duramycin hotspot, but appeared to be smaller in size upon visual inspection of the images (Fig. 3C and D). Of the 9 animals enrolled, 5 had myocardial ischemia in the left anterior coronary branch, and the remaining 4 had occlusion at the circumflex territory. Hot spot radioactivity uptake unambiguously identified all ischemic regions. An additional example, taken at 1 hr post-injection from an animal with a relatively small region of myocardial ischemia at the distal region in the circumflex territory, is shown in Fig. 4. Overall, signals at the focal uptake in ischemic regions were significantly above background. The ischemic-to-remote uptake ratios were 3.57 ± 0.74 and 3.69 ± 0.91 at 1 and 3 hours post-injection, respectively. Ischemic-to-lung ratios were 4.89 ± 0.85 and 4.93 ± 0.57, at 1 and 3 hours, respectively. Over the same period, there was a significant improvement in ischemic-to-liver ratios, from 2.05 ± 0.30 to 3.23 ± 0.78 ($P < 0.05$). No adverse effect associated with the injected radiopharmaceutical was seen.

Nuclear Medicine and Biology, Vol 41, No. 2 (February 2015): pg. 198-204. DOI.

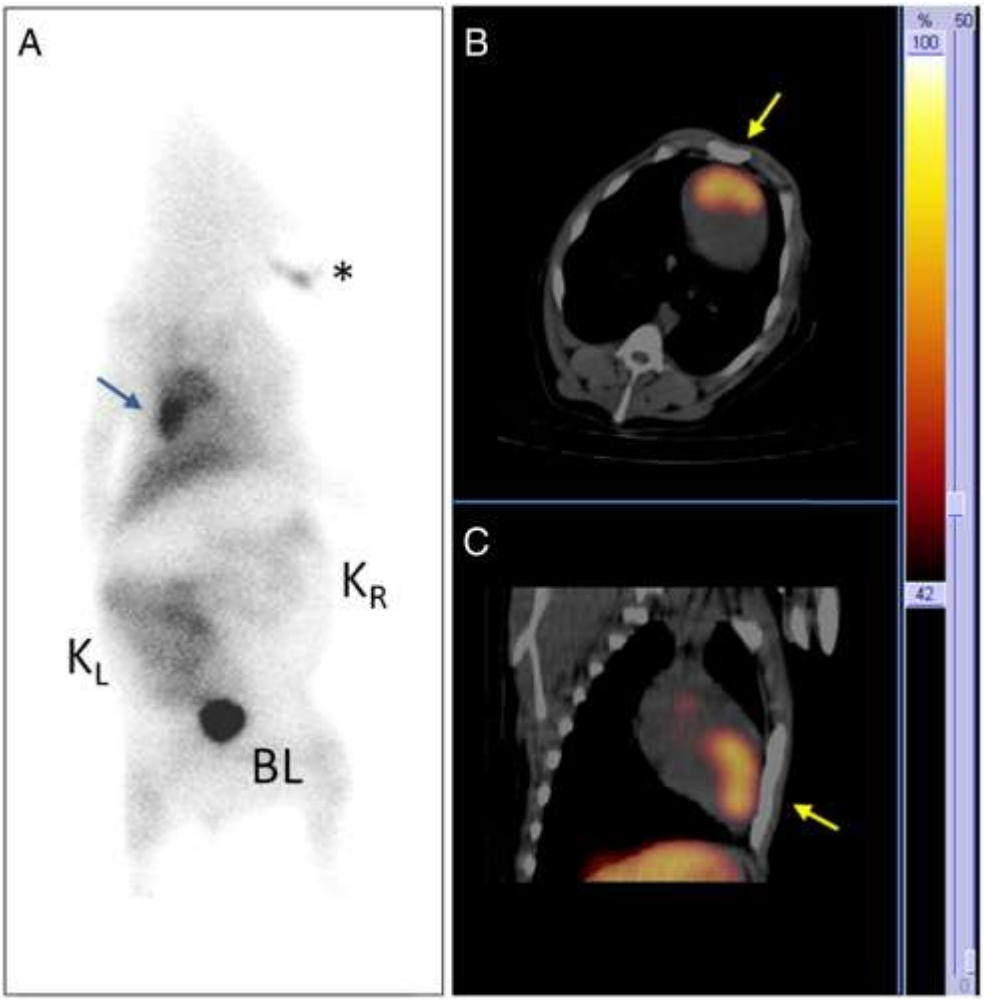

Fig. 2. Imaging ischemic myocardial injury using ^{99m}Tc-duramycin in a pig model of myocardial ischemia and reperfusion. (A) Whole-body anterior planar image acquired at 30 minutes post-injection. Radioactivity uptake in the ischemic heart region can be differentiated from the background, as marked by an arrow. Injection site via the ear vein is marked with an asterisk. Left and right kidneys are labeled as K_L and K_R, respectively. The bladder is marked as BL. (B and C) Short- and long-axial SPECT/CT fusion images acquired at 1 hour post-injection, with a hot spot ^{99m}Tc-duramycin uptake at the anterior left ventricular free wall (arrow). (D and E) Short- and long-axial images acquired at 3 hours from the same animal. Consecutive slices are shown in Supplementary Fig. 1 and Supplementary Fig. 2, for 1 and 3 hour data, respectively.

Nuclear Medicine and Biology, Vol 41, No. 2 (February 2015): pg. 198-204. DOI.

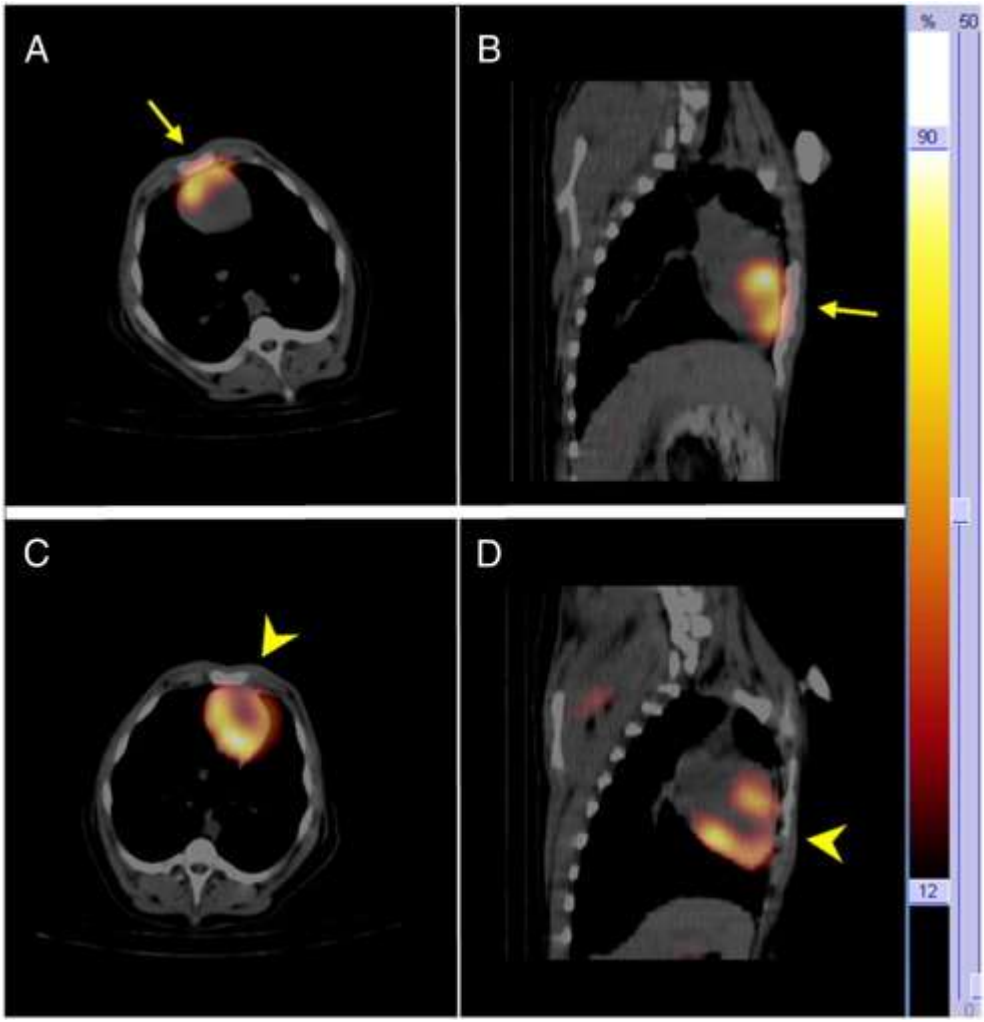

Fig. 3. A representative example of a relatively small, apical region of ischemic injury detected in SPECT/CT using ^{99m}Tc-duramycin. (A) Short-axial CT of the thorax. (B and C) A small area of ischemic and reperfusion injury was identified (arrows) at the apical region of the heart as a result of distal circumflex occlusion.

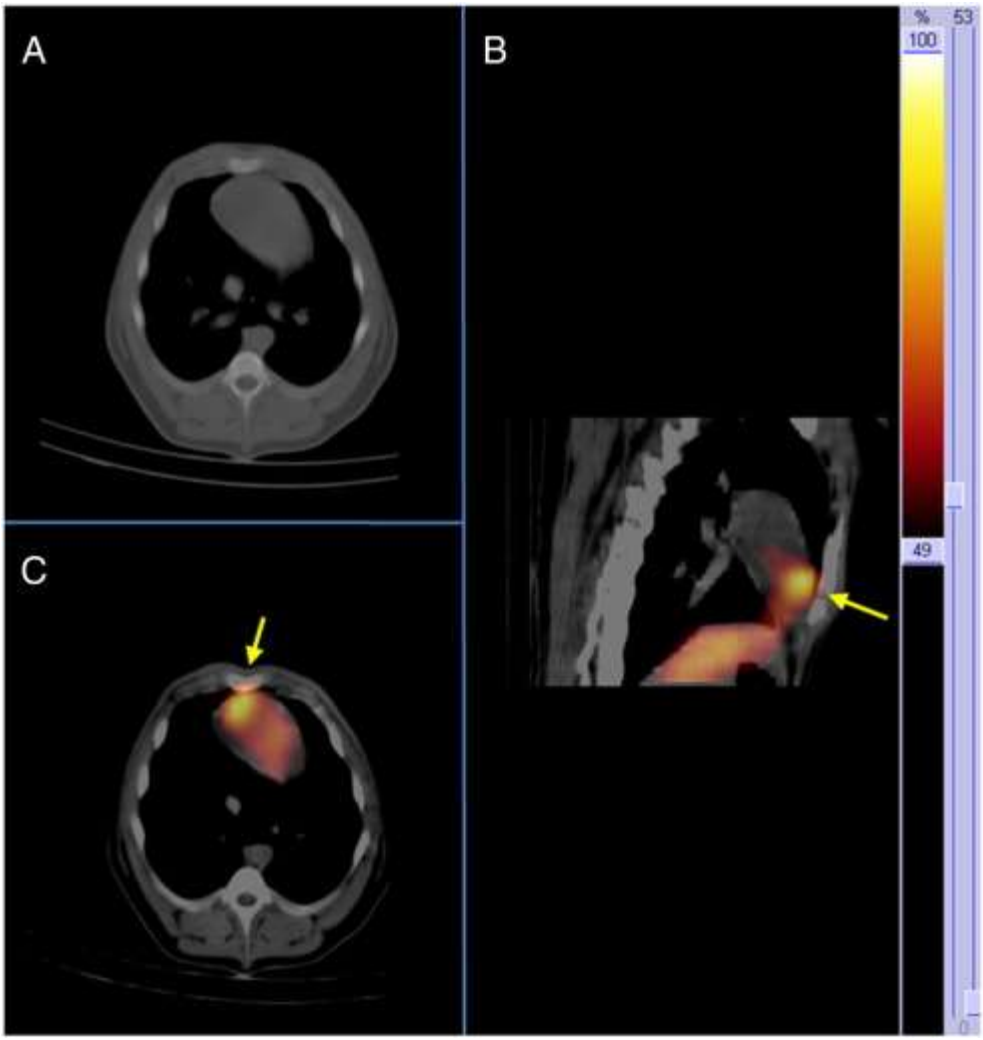

Fig. 4. Imaging small region of acute ischemic myocardial injury using ^{99m}Tc-duramycin. (A) Short-axial CT of the thorax. (B and C) A small area of ischemic and reperfusion damage is identified (arrows) at the apical region of the heart as a result of distal circumflex occlusion.

3.3. Post-mortem tissue analysis

The localization of radioactivity uptake in ischemic tissue was examined in post-mortem analysis. As shown in Fig. 5A, the location of hot spot radioactivity uptake was consistent with the perfusion territory of occluded coronary branch. The presence of high radioactivity was localized at TTC-deficient, infarcted myocardium as well as border regions. The total area positive for radioactivity was visually larger than the size of total infarcted (TTC-negative) tissues. These measurements were consistent with visibly larger ^{99m}Tc-

duramycin-positive regions in vivo versus perfusion defects in ^{99m}Tc-tetrofosmin scan. The percentage of nuclei with DNA damage characteristic of apoptotic cells in ischemic myocardium, as shown by TUNEL assay (Fig. 5B), was 28.04% ± 3.25% versus a baseline of 3.49% ± 1.83% in normal myocardium ($P < 0.001$). This was accompanied with a rise in cells at sub-G0 phase (4.62% ± 1.96% versus 0.50% ± 0.23% in normal myocardium, $P = 0.022$), which reflects necrotic cells that had reduced nucleic acid content due to compromised plasma membrane and cellular integrity. The relatively high percentage of apoptotic and necrotic cells was consistent with ischemic/reperfusion injury. Ultrastructural changes associated with ischemic tissue damages were documented using transmission electron microscopy, where features that are typical of apoptotic and necrotic cell death are present, including cytoplasm shrinkage, nuclear condensation and marginalization, and mitochondrial deformation (Fig. 5C). The presence of fragmented nuclei, myofibril degeneration and local hemorrhage, which are typical changes associated with ischemic injuries, are detected in H&E stained tissue sections (Fig. 5D).

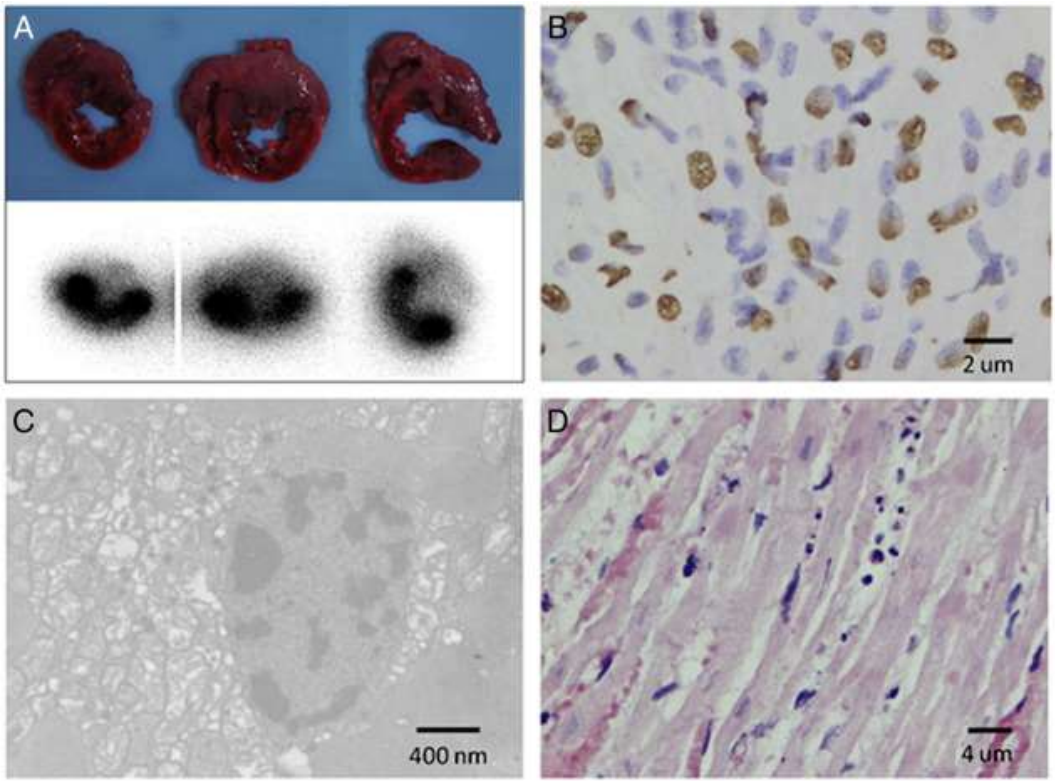

Nuclear Medicine and Biology, Vol 41, No. 2 (February 2015): pg. 198-204. DOI.

Fig. 5. Histological analyses. (A) TTC stained (upper) and autoradiography (lower) of the same short-axial heart sections. (B) TUNEL staining of tissue harvested from the periphery of the ischemic core. (C) Ultrastructural changes associated with ischemia/reperfusion injury, as identified with transmission electron microscopy. (D) H&E staining of damaged myocardium at the ischemic zone.

4. Discussion

There are a number of significant findings from the current investigation. As demonstrated in a large animal model, the *in vivo* clearance profile of ^{99m}Tc-duramycin is appropriate for imaging in the cardiovascular system. An avid uptake in the target tissue combined with a low background enabled the noninvasive imaging of ischemic/reperfusion myocardial injury in the acute phase as early as 30 minutes after injection. In addition to an uptake in infarcted myocardium, ^{99m}Tc-duramycin binding to ischemic-but-noninfarct tissues indicated that it was effective in detecting ischemically injured myocardium.

Molecular features of ^{99m}Tc-duramycin are unique for having both a robust binding mechanism and a favorable clearance profile. Antibodies and larger proteins have exquisite binding properties but suboptimal clearance for *in vivo* imaging. On the other hand, while short peptides in general have superior pharmacokinetics, they lack structurally-defined binding modules such as that of immunoglobulin fold. The underlying conundrum is that a strong molecular recognition mechanism requires a well-defined binding structure, which often necessitates extensive scaffolding only afforded in large proteins. Currently, the roles of peptide-based imaging agents are predominantly confined to ligands that are recognized and sequestered by cognate receptors. The molecular features of duramycin combine the two extremes in the spectrum of binding-versus-size relationship. The overall structure of duramycin with a stereospecific binding pocket is accomplished with only 19 amino acids (molecular weight 2 kDa), making duramycin and its structural derivatives uniquely situated for imaging applications.

With accumulating evidence, the pathological externalization of PE is being established as an imaging marker for tissue/cellular injuries.[10,11,15,16,17] The sarcolemma of cardiomyocytes is a rich source of PE, which when externalized to the cell surface constitutes an

abundant molecular target. In contrast to conventional infarct-avid imaging approaches, membrane phospholipid scrambling occurs in both apoptosis and necrosis. In cells under severe ischemia, their ability to maintain proper phospholipid asymmetry is compromised, and the transbilayer redistribution of aminophospholipids provides an additional source of target for detection.[18,13,19] As such, membrane phospholipid scrambling as a biomarker reflects global injury instead of infarction *per se*. This was consistent with the current finding where the myocardial region positive for ^{99m}Tc-duramycin uptake was visually more expansive than the infarct alone. When fully established, the ability to accurately assess the full extent of myocardial injury is likely to lead to a better diagnostic marker for ischemic coronary syndromes, with prognostic predictive value for adverse cardiac events like heart failure and the risk for arrhythmia.

5. Conclusion

The clearance of intravenously injected ^{99m}Tc-duramycin was predominantly via the renal/urinary tract with relatively low systemic and hepatic background in a large animal model. These *in vivo* properties were suitable for imaging applications for the cardiovascular system. Data from the porcine model of myocardial ischemia and reperfusion indicated that the uptake of ^{99m}Tc-duramycin enabled the detection of ischemically-injured myocardial tissues effectively.

Conflict of interest statement

The authors declare that they have no conflict of interest.

Acknowledgment

This research was supported by grants from National Natural Science Foundation of China (81171383, 81071176, 81371586, 91229127, 81070194), Department of Veterans Affairs, and the National Institute of Health (1R01HL102085).

References

[1] P. Williamson, R.A. Schlegel. Transbilayer phospholipid movement and the clearance of apoptotic cells. *Biochim Biophys Acta*, 1585 (2002), pp. 53–63

[2] K. Emoto, N. Toyama-Sorimachi, H. Karasuyama, *et al.* Exposure of phosphatidylethanolamine on the surface of apoptotic cells. *Exp Cell Res*, 232 (1997), pp. 430–434

[3] M. Zhao, X. Zhu, S. Ji, *et al.* 99mTc-labeled C2A domain of synaptotagmin I as a target-specific molecular probe for noninvasive imaging of acute myocardial infarction. *J Nucl Med*, 47 (2006), pp. 1367–1374

[4] J.F. Tait, C. Smith, F.G. Blankenberg. Structural requirements for in vivo detection of cell death with 99mTc-annexin V. *J Nucl Med*, 46 (2005), pp. 807–815

[5] L. Hofstra, I.H. Liem, E.A. Dumont, *et al.* Visualisation of cell death in vivo in patients with acute myocardial infarction. *Lancet*, 356 (2000), pp. 209–212

[6] F.G. Blankenberg, P.D. Katsikis, J.F. Tait, *et al.* In vivo detection and imaging of phosphatidylserine expression during programmed cell death. *Proc Natl Acad Sci U S A*, 95 (1998), pp. 6349–6354

[7] A. Flotats, I. Carrió. Non-invasive in vivo imaging of myocardial apoptosis and necrosis. *Eur J Nucl Med Mol Imaging*, 30 (2003), pp. 615–630

[8] F. Hayashi, K. Nagashima, Y. Terui, *et al.* The structure of PA48009: the revised structure of duramycin. *J Antibiot (Tokyo)*, 43 (1990), pp. 1421–1430

[9] N. Zimmermann, S. Freund, A. Fredenhagen, *et al.* Solution structures of the lantibiotics duramycin B and C. *Eur J Biochem*, 216 (1993), pp. 419–428

[10] M. Zhao, Z. Li, S. Bugenhagen. ^{99m}Tc-labeled duramycin as a novel phosphatidylethanolamine-binding molecular probe. *J Nucl Med*, 49 (2008), pp. 1345–1352

[11] S. Audi, Z. Li, J. Capacete, *et al.* Understanding the in vivo uptake kinetics of a phosphatidylethanolamine-binding agent (99 m)Tc-duramycin. *Nucl Med Biol*, 39 (2012), pp. 821–825

[12] K. Iwamoto, T. Hayakawa, *et al.* Curvature-dependent recognition of ethanolamine phospholipids by duramycin and cinnamycin. *Biophys J*, 93 (2007), pp. 1608–1619

[13] J.A. Post, A.J. Verkleij, G.A. Langer. Organization and function of sarcolemmal phospholipids in control and ischemic/reperfused cardiomyocytes. *J Mol Cell Cardiol*, 27 (1995), pp. 749–760

[14] M. Zhao, Z. Li. A single-step kit formulation for the (99 m)Tc-labeling of HYNIC-Duramycin. *Nucl Med Biol*, 39 (2012), pp. 1006–1011

[15] A.V. Clough, S.H. Audi, S.T. Haworth, D.L. Roerig. Differential lung uptake of ^{99m}Tc-hexamethylpropyleneamine oxime and ^{99m}Tc-duramycin in the chronic hyperoxia rat model. *J Nucl Med*, 53 (2012), pp. 1984–1991

[16] Y. Zhang, G.D. Stevenson, C. Barber, L.R. Furenlid, H.H. Barrett, J.M. Woolfenden, *et al.* Imaging of rat cerebral ischemia–reperfusion injury using(99 m)Tc-labeled duramycin. *Nucl Med Biol*, 40 (2013), pp. 80–88

[17] S.E. Johnson, Z. Li, Y. Liu, J.E. Moulder, M. Zhao. Whole-body imaging of high-dose ionizing irradiation-induced tissue injuries using ^{99m}Tc-duramycin. *J Nucl Med*, 54 (2013), pp. 1397–1403

[18] R.J. Musters, E. Otten, E. Biegelmann, J. Bijvelt, J.J. Keijzer, J.A. Post, *et al.* Loss of asymmetric distribution of sarcolemmal phosphatidylethanolamine during simulated ischemia in the isolated neonatal rat cardiomyocyte. *Circ Res*, 73 (1993), pp. 514–523

[19] H. Kenis, H.R. Zandbergen, L. Hofstra, *et al.* Annexin A5 uptake in ischemic myocardium: demonstration of reversible phosphatidylserine externalization and feasibility of radionuclide imaging. J Nucl Med, 51 (2010), pp. 259–267

Correspondence to: B. Zhu, Department of Nuclear Medicine, Wuxi People's Hospital Affiliated to Nanjing Medical University, 299 Qingyang Road, Wuxi 214023, China. Tel.:+86 510 85350384.

Correspondence to: H. Zhu, State Key Laboratory of Bioactive Substance and Function of Natural Medicines, Institute of Materia Medica, Peking Union Medical College & Chinese Academy of Medical Sciences, Xiannongtan Road, Beijing 100050, China. Tel.: + 86 10 63188106.

Correspondence to: M. Zhao, Feinberg Cardiovascular Research Institute, Department of Medicine, Northwestern University, 303 E. Chicago Avenue, Chicago, IL 60611, USA. Tel.: + 1 312 503 3226.

The following are the supplementary data related to this article.

Supplementary Fig. 1.

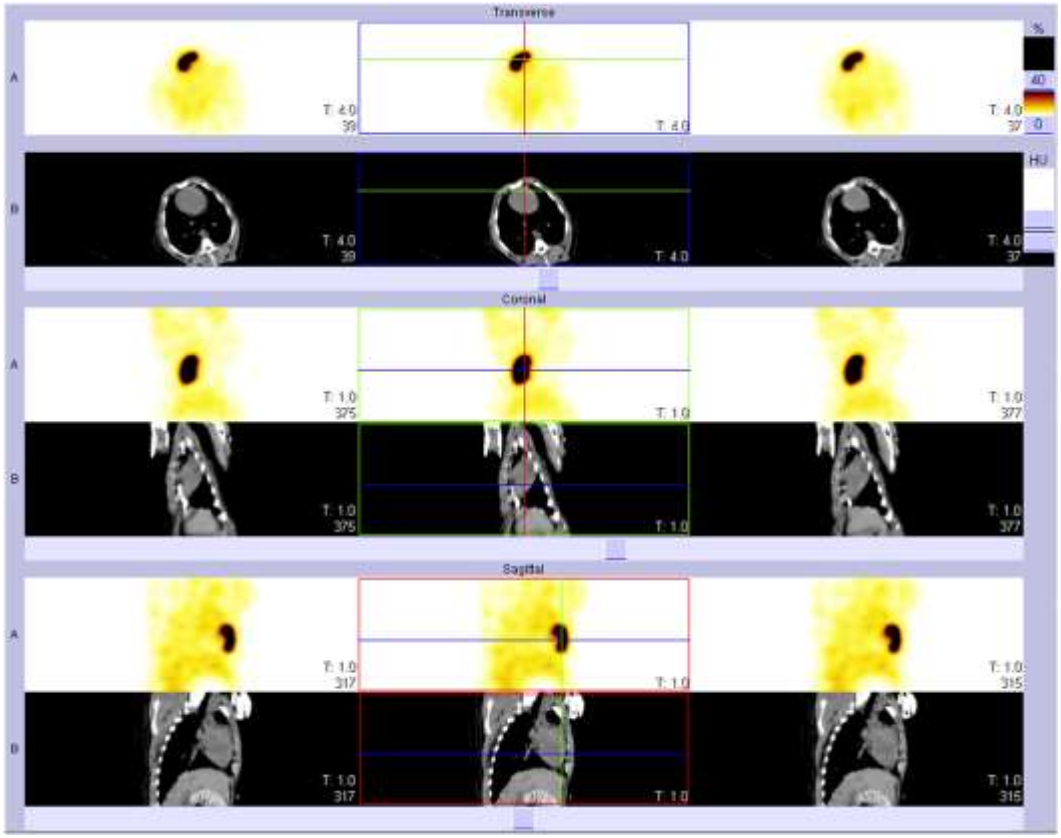

Consecutive slices in axial, sagittal and coronal SPECT/CT data acquired at 1 hr post injection.

Nuclear Medicine and Biology, Vol 41, No. 2 (February 2015): pg. 198-204. DOI.

Supplementary Fig. 2.

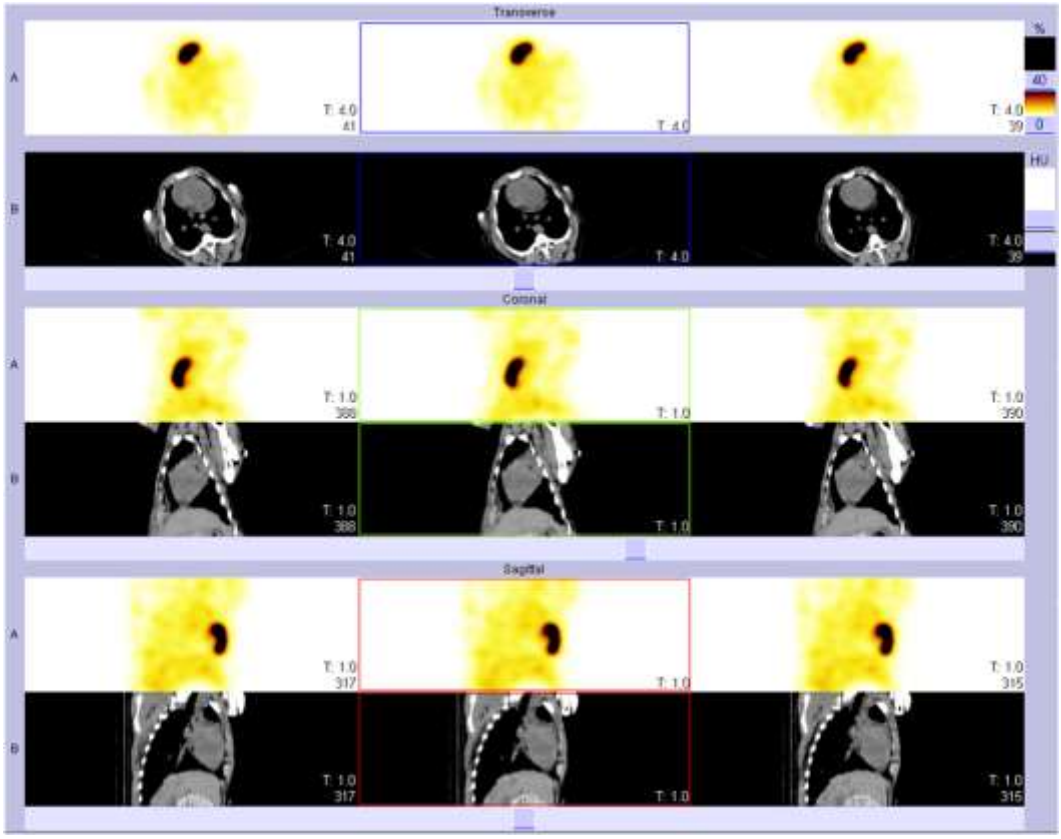

Consecutive slices in axial, sagittal and coronal SPECT/CT data acquired at 3 hr post injection.

Nuclear Medicine and Biology, Vol 41, No. 2 (February 2015): pg. 198-204. DOI.